

Role of anion exchangers in Cl^- and HCO_3^- secretion by the human airway epithelial cell line Calu-3

Dusik Kim,¹ Juyeon Kim,¹ Beáta Burghardt,² Len Best,³ and Martin C. Steward¹

¹Faculty of Life Sciences, University of Manchester, Manchester, United Kingdom; ²Department of Oral Biology, Semmelweis University, Budapest, Hungary; and ³Faculty of Medicine and Human Sciences, University of Manchester, Manchester, United Kingdom

Submitted 19 March 2014; accepted in final form 30 May 2014

Kim D, Kim J, Burghardt B, Best L, Steward MC. Role of anion exchangers in Cl^- and HCO_3^- secretion by the human airway epithelial cell line Calu-3. *Am J Physiol Cell Physiol* 307: C208–C219, 2014. First published June 4, 2014; doi:10.1152/ajpcell.00083.2014.—Despite the importance of airway surface liquid pH in the lung's defenses against infection, the mechanism of airway HCO_3^- secretion remains unclear. Our aim was to assess the contribution of apical and basolateral $\text{Cl}^-/\text{HCO}_3^-$ exchangers to Cl^- and HCO_3^- transport in the Calu-3 cell line, derived from human airway submucosal glands. Changes in intracellular pH (pH_i) were measured following substitution of Cl^- with gluconate. Apical Cl^- substitution led to an alkalization in forskolin-stimulated cells, indicative of $\text{Cl}^-/\text{HCO}_3^-$ exchange. This was unaffected by the anion exchange inhibitor DIDS but inhibited by the CFTR blocker CFTR_{inh}-172, suggesting that the HCO_3^- influx might occur via CFTR, rather than a solute carrier family 26 (SLC26) exchanger, as recently proposed. The anion selectivity of the recovery process more closely resembled that of CFTR than an SLC26 exchanger, and quantitative RT-PCR showed only low levels of SLC26 exchanger transcripts relative to CFTR and anion exchanger 2 (AE2). For pH_i to rise to observed values (~ 7.8) through HCO_3^- entry via CFTR, the apical membrane potential must reverse to at least +20 mV following Cl^- substitution; this was confirmed by perforated-patch recordings. Substitution of basolateral Cl^- evoked a DIDS-sensitive alkalization, attributed to $\text{Cl}^-/\text{HCO}_3^-$ exchange via AE2. This appeared to be abolished in forskolin-stimulated cells but was unmasked by blocking apical efflux of HCO_3^- via CFTR. We conclude that Calu-3 cells secrete HCO_3^- predominantly via CFTR, and, contrary to previous reports, the basolateral anion exchanger AE2 remains active during stimulation, providing an important pathway for basolateral Cl^- uptake.

cystic fibrosis transmembrane conductance regulator; airway surface liquid; cystic fibrosis; intracellular pH; bicarbonate; $\text{Cl}^-/\text{HCO}_3^-$ exchange; anion exchanger 2; SLC26A4 (pendrin)

AIRWAY SURFACE LIQUID (ASL) plays an important protective role in clearing the upper airways of inhaled particulate matter and microorganisms (3). It consists of a thin aqueous film supporting a mucin raft that traps dust and pathogens and is swept toward the pharynx by cilia (9). ASL must be continuously replenished by secretions derived largely from the submucosal glands in the upper airways to counter the effects of evaporation and expectoration. The electrolytes are thought to be secreted mainly by the serous cells, a major site of cystic fibrosis transmembrane conductance regulator (CFTR) expression (8, 25, 53). The depth of the aqueous layer is determined by the balance between Cl^- secretion and Na^+ reabsorption (4). Both of these processes are disturbed in cystic fibrosis

(CF), with the result that the depth of the aqueous layer is reduced, mucociliary clearance is impaired, the mucus layer is less well hydrated, and the airways become infected and inflamed (3, 44).

ASL is near neutral pH (pH 6.6–7.0) and becomes slightly more acidic in CF (5, 10, 60), which increases the susceptibility of the airway surface to infection (42). Studies on isolated submucosal glands and airway epithelial cells in primary culture indicate that CFTR is essential for fluid and HCO_3^- secretion (26, 59, 63). In addition to its role in ASL pH regulation, the secreted HCO_3^- specifically facilitates the expansion and solubilization of secreted mucin granules (14, 45, 46); thus a reduction of HCO_3^- secretion, as well as fluid volume, may contribute to the pathophysiology of CF. Understanding the mechanism of HCO_3^- secretion by human airway serous cells is therefore of prime importance.

The Calu-3 cell line was derived from a human lung carcinoma and has proved to be a useful experimental model for studying CFTR-dependent HCO_3^- secretion (54). Its phenotype resembles that of serous cells of the submucosal glands, it expresses abundant CFTR (15, 57), and it has been shown to secrete a moderately HCO_3^- -rich fluid in vitro (11, 21, 55).

By analogy with other HCO_3^- -secreting epithelia, such as the intestine and pancreatic duct, the secretory mechanism might be expected to involve the combined activity of CFTR and an apical $\text{Cl}^-/\text{HCO}_3^-$ exchanger of solute carrier family 26 (SLC26), typically SLC26A3 or SLC26A6 (31, 66). The CFTR channel itself has a relatively low permeability to HCO_3^- (19, 32, 39, 43), so the SLC26 $\text{Cl}^-/\text{HCO}_3^-$ exchangers are thought to provide the main pathway for HCO_3^- secretion. Indeed, our own preliminary studies, examining the effect of extracellular Cl^- substitution on intracellular pH (pH_i) (27, 35), and similar work by Garnett et al. (11), have pointed to the possible involvement of the anion exchanger pendrin (SLC26A4) in HCO_3^- secretion across the apical membrane of Calu-3 cells. In this model, Cl^- secretion via CFTR defines the secretory (volume) flow rate, while the subsequent exchange of secreted Cl^- for intracellular HCO_3^- via pendrin defines the HCO_3^- concentration of the secreted fluid (11).

There is, however, a substantial body of evidence, much of it from Ussing chamber studies, to suggest that HCO_3^- secretion at the apical membrane is mediated mainly by CFTR, rather than by an associated exchanger such as pendrin. The secretory flux of HCO_3^- (1) appears to be directly related to its electrochemical driving force at the apical membrane, 2) is abolished by CFTR blockers, 3) is insensitive to the anion exchange inhibitor DIDS, and 4) does not require Cl^- in the apical bathing solution (6, 18, 20, 29, 55).

Address for reprint requests and other correspondence: M. C. Steward, Faculty of Life Sciences, Univ. of Manchester, Michael Smith Bldg., Manchester, M13 9PT, UK (e-mail: martin.steward@manchester.ac.uk).

The present study investigates these alternative models, with a focus on two aspects. We test whether pH_i changes observed in response to extracellular anion substitution, and previously attributed to apical $\text{Cl}^-/\text{HCO}_3^-$ exchange via pendrin, can instead be explained by electrical coupling of Cl^- and HCO_3^- fluxes via CFTR. We also reexamine the role of the basolateral $\text{Cl}^-/\text{HCO}_3^-$ exchanger in the light of two other conflicting reports, one suggesting that basolateral AE2 has a key role in HCO_3^- -dependent Cl^- secretion (16) and the other suggesting the opposite, i.e., that its activity is suppressed during cAMP stimulation to maximize HCO_3^- secretion (12).

MATERIALS AND METHODS

Materials

Cell culture media were obtained from Invitrogen (Life Technologies, Paisley, UK), 2',7-bis-(2-carboxyethyl)-5-(and 6)-carboxyfluorescein acetoxymethyl ester (BCECF-AM) from Molecular Probes (Life Technologies, Paisley, UK), and CFTR_{inh}-172 from Calbiochem (Merck Biosciences, Nottingham, UK). All other compounds were obtained from Sigma-Aldrich (Dorset, UK).

Cell Culture

Calu-3 cells (HTB-55, American Type Culture Collection) were obtained from LGC Promochem (Teddington, UK). Cells were grown in Eagle's minimum essential medium supplemented with fetal bovine serum (10%), L-glutamine (2 mM), nonessential amino acids (0.1 mM), sodium pyruvate (1 mM), penicillin (100 U/ml), and streptomycin (0.1 mg/ml). Cells were incubated at constant humidity in 5% CO_2 at 37°C and subcultured at weekly intervals by trypsinization at a 1:10 ratio. For experiments, cells were seeded onto Transwell clear polyester inserts (6.5 mm diameter, 0.4 μm pore size; Corning Costar, Buckinghamshire, UK) and grown for ≥ 10 days before they were used to establish a polarized monolayer. Transepithelial resistance under these conditions was $\sim 300 \Omega\text{-cm}^2$ after correction for solution and filter resistances.

Measurement of pH_i

Calu-3 cells cultured on Transwell inserts were loaded with the pH-sensitive dye BCECF by incubation with the acetoxymethyl ester BCECF-AM (5 μM) in a HCO_3^- -buffered solution for 30 min in 5% CO_2 at 37°C. After the loading period, inserts were mounted in a Perspex perfusion chamber on the stage of an inverted fluorescence microscope (Nikon Diaphot TMD). The fluid volumes in the apical and basolateral hemichambers were ~ 100 and 80 μl , respectively, and the flow rate through each was 1.5 ml/min. Solutions were prewarmed to 37°C, and the temperature of the chamber was maintained at 37°C by a thermostatically controlled, heated platform (Warner Instruments, Hamden, CT). Cells were excited alternately at 440 and 490 nm for 1 s at each wavelength. Fluorescence emitted by BCECF was measured photometrically at 530 nm (Cairn Research, Faversham, UK). pH_i was calculated from the ratio of fluorescence at 490 nm to fluorescence at 440 nm using calibration data obtained *in situ* by the nigericin- K^+ method (64).

A HEPES-buffered solution (in mM: 117 NaCl, 5 KCl, 1 CaCl_2 , 1 MgSO_4 , 5 NaHEPES, 5 HEPES, and 10 D-glucose) was used as the standard solution for nominally HCO_3^- -free experiments and was gassed with 100% O_2 . For experiments performed in the presence of HCO_3^- , the standard HCO_3^- -buffered solution contained (in mM) 96 NaCl, 5 KCl, 1 CaCl_2 , 1 MgCl_2 , 10 D-glucose, and 25 NaHCO_3 and was bubbled with 95% O_2 -5% CO_2 . In solutions containing NH_4Cl , 20 mM NaCl was replaced with equimolar NH_4Cl . Na^+ was isosmotically replaced with equimolar N-methyl-D-glucamine (NMDG⁺) in all Na^+ -free solutions. The Na^+ -free, HCO_3^- -buffered solution contained 25 mM NMDG- HCO_3 in place of NaHCO_3 . This was

prepared by gassing a 1 M solution of NMDG overnight with 100% CO_2 . For the anion substitution experiments, the HCO_3^- -buffered control solution contained (in mM) 116 NaCl, 5 KCl, 1 CaCl_2 , 1 MgSO_4 , 2.8 NaHEPES, 2.2 HEPES, 10 D-glucose, and 25 NaHCO_3 . In the Cl^- -free solutions, Cl^- was replaced with equimolar gluconate, and the Ca^{2+} concentration was raised to 4 mM to compensate for the chelation of Ca^{2+} by gluconate. For the anion selectivity experiments, Cl^- was replaced with equimolar I^- and formate (HCOO^-) and by SO_4^{2-} and succinate at one-half of the Cl^- concentration, with isotonicity maintained by addition of 53 mM mannitol.

Perforated-Patch Experiments

Calu-3 cells plated on poly-L-lysine-coated coverslips were placed in a patch-clamp chamber (35 mm diameter) that was constantly perfused at a rate of ~ 2 ml/min with a bath solution containing (in mM) 115 NaCl, 25 NaHEPES, 1 MgCl_2 , 1.2 CaCl_2 , 4 KCl, 10 HEPES, and 4 glucose (pH 7.4, HEPES-buffered solution) or 115 NaCl, 25 NaHCO_3 , 1 MgCl_2 , 1.2 CaCl_2 , 4 KCl, 10 HEPES, and 4 glucose (pH 7.4, HCO_3^- -buffered solution). Perfusion buffers containing HCO_3^- were bubbled with 95% O_2 -5% CO_2 .

Membrane potential was recorded with an EPC-7 amplifier (List, Darmstadt, German) in individual Calu-3 cells using the perforated-patch technique under zero current-clamp conditions. They were studied acutely after dissociation, expressed functional CFTR, and were effectively short-circuited under these experimental conditions. The basic pipette solution contained (in mM) 135 KCl, 5 NaCl, 1 MgCl_2 , 1.2 CaCl_2 , 4 KCl, 10 HEPES, and 4 glucose (pH 7.2). Pipette tips were filled with the gramicidin D-containing pipette solution. The reference electrode was connected to the bath solution via an agar-KCl (140 mM) bridge, in experiments in which the external Cl^- was removed, to prevent generation of a junction potential. Changes in the membrane potential of the Calu-3 cells were recorded with pCLAMP 6 software (Axon Instruments), and data were acquired at 1-s intervals using LabVIEW 8.2 software (National Instruments, Austin, TX). All patch-clamp experiments were carried out at room temperature (23–25°C).

RNA Isolation and Quantification

Total RNA was isolated from Calu-3 cells using the RNeasy Micro Kit (Qiagen, West Sussex, UK) according to the manufacturer's instructions. Prior to the analysis of gene expression, purified total RNA quality and quantity were evaluated with a spectrophotometer (model ND-1000, NanoDrop Technologies, Wilmington, DE). Values of 1.9–2.1 for the ratio of OD at 260 nm to OD at 280 nm were considered to indicate adequate purity. Purified RNA was stored at -80°C prior to use for further experiments.

RT-PCR

Single-strand cDNA synthesis was performed on high-quality, purified RNA samples using a high-capacity RNA-to-cDNA kit (Applied Biosystems, Warrington, UK). The incubation was performed at 37°C for 60 min, stopped at 95°C for 5 min, and then held at 4°C in a thermal cycler. The PCR products were then electrophoresed on 1.5% agarose-Tris-acetate-EDTA gel incorporating ethidium bromide (0.5 mg/ml) in 0.5 \times agarose-Tris-acetate-EDTA running buffer at 110 V. After electrophoresis, the DNA bands were visualized and photographed under UV light using a gel documentation and analysis system (Uvitec, Cambridge, UK). A 100-bp DNA ladder (Promega, Madison, WI) was used to determine the size of the bands.

Quantitative PCR

Real-time quantitative PCRs (qPCRs) were performed using TaqMan gene expression assays (Applied Biosystems). Ten microliters of master mix and 1 μl of pre-designed primers (from inventoried assays that had been validated by the manufacturer; Table 1) were added to

Table 1. Gene-specific primers used for RT-PCR and real-time quantitative PCR using TaqMan gene expression assays

Gene	Assay ID No.	Accession No.	Amplicon Length, bp
CFTR	Hs00357011_m1	NM_000492.3	93
SLC4A2 (AE2)	Hs015867776_m1	NM_003040.3	131
SLC26A2	Hs00164423_m1	NM_000112.3	73
SLC26A3	Hs00230798_m1	NM_000111.2	117
SLC26A4	Hs00166504_m1	NM_000441.1	89
SLC26A6	Hs00370470_m1	NM_022911.2, NM_134263.2, NM_134426.2, NM_001040454.1	81
SLC26A7	Hs01104163_m1	NM_134266.1, NM_052832.2	85
SLC26A9	Hs00369451_m1	NM_134325.2, NM_052934.3, NM_001142600.1	67

each cDNA sample. The plates were analyzed in a real-time PCR thermocycler using SDS software (model 7500, Applied Biosystems). Amplification was performed with the following cycle parameters: 10 min at 95°C and 40 cycles of 15 s at 95°C and 60 s at 60°C. The threshold value was manually adjusted to pass through the linear portion of the curve corresponding to the exponential phase of amplification. The raw cycle threshold (C_T) values obtained from the TaqMan assays were normalized to 18S rRNA using the $2^{-\Delta\Delta C_T}$ method (33) to compare the mRNA expression levels of the individual transporters.

Statistical Analysis

Individual measurements are presented as means \pm SE, where n indicates the number of experiments. Averaged time courses of pH_i changes from n identical experiments are shown as a solid line representing the mean and dashed lines representing SE. To assess statistical significance, Student's t -test or ANOVA followed by a post hoc Tukey's test was carried out using Excel and GraphPad Prism 6, respectively. $P < 0.05$ was chosen as the threshold for statistical significance. Rates of change in pH_i were estimated by linear regression over a 1-min period during the first 2 min of pH_i recovery.

RESULTS

Basolateral Cl^-/HCO_3^- Exchange

Previous studies on Calu-3 cells indicate that the Cl^-/HCO_3^- exchanger AE2 is expressed at the basolateral membrane (16, 34, 55). To confirm this, we studied the effect of removing Cl^- from the basolateral perfusate in the presence of HCO_3^- . The expectation was that pH_i would increase as a result of HCO_3^- uptake via AE2, driven by the reversed Cl^- concentration gradient. As shown in Fig. 1A, substitution of basolateral Cl^- with gluconate caused a significant increase in pH_i ($\Delta pH_i = 0.27 \pm 0.062$, $P < 0.05$, paired Student's t -test).

To determine whether this alkalization was due to Cl^-/HCO_3^- exchange via AE2, the experiment was repeated in the presence of basolateral DIDS, an anion exchanger inhibitor (Fig. 1B). As expected, 100 μM DIDS completely inhibited the alkalization [$\Delta pH_i = -0.04 \pm 0.02$, $n = 6$, $P > 0.05$ compared with zero (by 1-sample t -test)], consistent with the presence of a DIDS-sensitive anion exchanger at the basolateral membrane.

Apical Cl^-/HCO_3^- Exchange

The presence or absence of an anion exchanger at the apical membrane of Calu-3 cells has become the subject of some debate (11, 50, 55). We therefore examined the effect of Cl^- substitution in the apical bath solution. Figure 1C shows that when Cl^- was replaced with gluconate at the apical membrane, there was no significant increase in pH_i ($\Delta pH_i = 0.038 \pm$

0.023 , $n = 12$, $P > 0.05$). This suggests that in unstimulated cells there is no measurable anion exchanger activity at the apical membrane.

However, HCO_3^- secretion by Calu-3 cells is markedly increased in response to cAMP stimulation. To investigate whether an apical exchanger becomes active following elevation of intracellular cAMP, forskolin (10 μM) and IBMX (100 μM) were applied 5 min prior to the Cl^- substitution period. As observed by others (17), cAMP stimulation alone elicited a small drop in pH_i to a new steady-state value ($\Delta pH_i = -0.18 \pm 0.01$, $n = 7$; Fig. 2). This drop is most likely due to a transient imbalance between the increased HCO_3^- efflux across the apical membrane and the uptake of HCO_3^- via $Na^+-HCO_3^-$ cotransporter NBC1 (and/or extrusion of H^+ via Na^+/H^+ exchanger NHE1) at the basolateral membrane. A new steady state is only achieved when these fluxes are again balanced at the slightly lower pH_i value.

As shown in Fig. 2A, removal of Cl^- at the apical membrane of cAMP-stimulated Calu-3 cells resulted in a large increase in pH_i ($\Delta pH_i = 0.46 \pm 0.14$, $n = 9$). Conversely, when basolateral Cl^- was substituted (Fig. 2B), the increase in pH_i that had been observed in unstimulated conditions (Fig. 1A) was greatly reduced by pretreatment with forskolin and IBMX. Taken at face value, these results, summarized in Fig. 2C, suggest that elevation of intracellular cAMP activates an anion exchanger at the apical membrane and suppresses anion exchange at the basolateral membrane, as reported elsewhere (11).

To investigate whether the alkalization induced by apical Cl^- substitution in the stimulated cells was due to the activity of an apical anion exchanger, the cells were pretreated with 100 μM DIDS. As shown in Fig. 2D, apical application of DIDS had only a small effect on the alkalization ($\Delta pH_i = 0.29 \pm 0.13$, not significantly different from the value obtained in the absence of DIDS). This was in marked contrast to the complete inhibition of basolateral Cl^-/HCO_3^- exchange by DIDS shown in Fig. 1B.

One possible explanation for these results is that Calu-3 cells express an apical anion exchanger that is activated by cAMP and is relatively insensitive to DIDS. It could, for example, be a member of the SLC26 family of anion transporters, which are widely expressed at the apical membrane of secretory epithelia.

Selectivity of Anion Exchange at the Apical Membrane

Members of the SLC26 family transport a diverse range of monovalent and divalent anions (7, 36). The next series of experiments tested the anion selectivity of the apical anion exchanger in cAMP-stimulated Calu-3 cells. Instead of returning Cl^- to the apical perfusate after the Cl^- -free period, alternative anions were applied to determine whether they

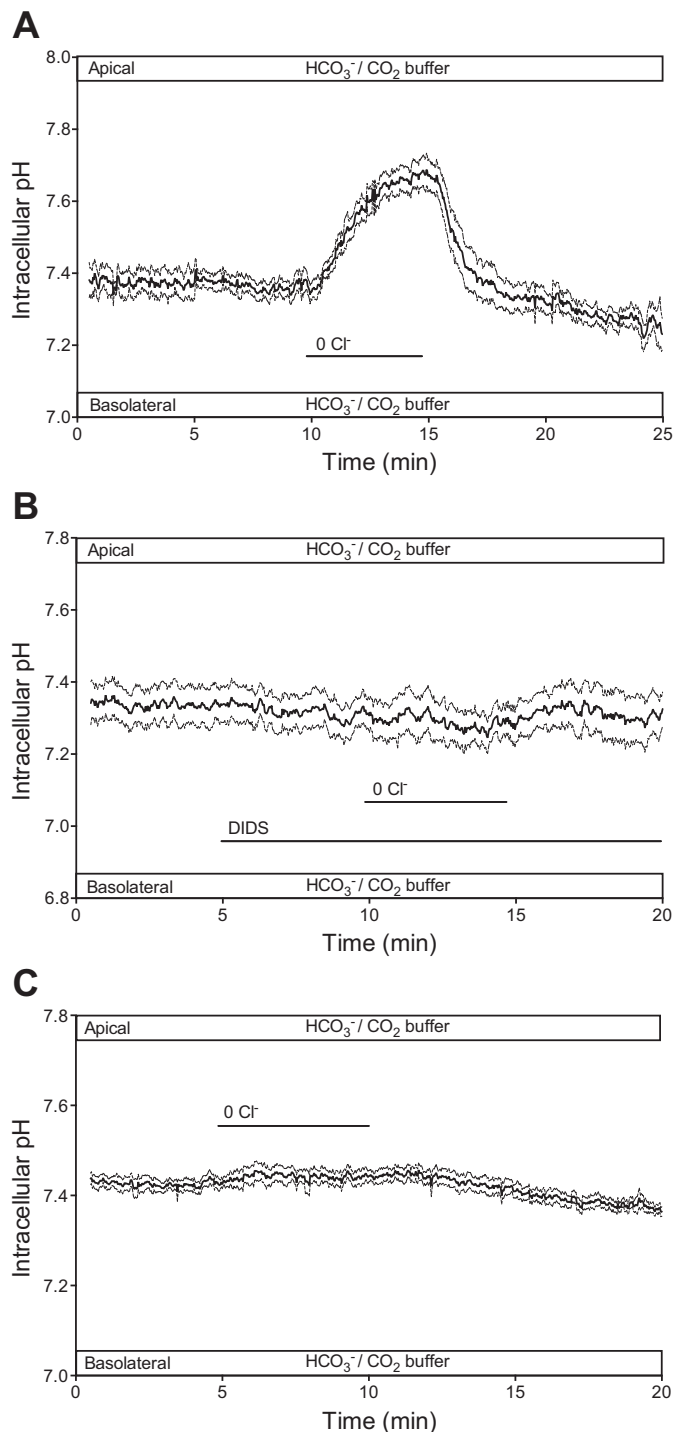


Fig. 1. Effects of apical and basolateral Cl⁻ substitution on intracellular pH (pH_i) in unstimulated Calu-3 cells in the presence of HCO₃⁻. Cells were superfused with a HCO₃⁻-buffered solution, and apical or basolateral Cl⁻ was replaced with gluconate. *A*: changes in pH_i in response gluconate replacement of Cl⁻ at the basolateral membrane ($n = 7$). *B*: inhibitory effect of DIDS (100 μM) on the response to basolateral Cl⁻ substitution ($n = 6$). *C*: effect of apical Cl⁻ substitution ($n = 12$). Solid lines represent averaged pH_i time course from n identical experiments, and dashed lines represent SE. Horizontal bar labeled 0 Cl⁻ indicates period of Cl⁻ substitution.

would support exchange with intracellular HCO₃⁻, thereby returning pH_i to its normal value. As shown in Fig. 3A, I⁻ was able to quickly restore pH_i to normal after gluconate substitution of apical Cl⁻, suggesting that the apical anion exchanger is also able to transport I⁻. The rate of recovery of pH_i was $-0.13 \pm 0.027 \text{ min}^{-1}$ ($n = 6$), approximately one-half of the value obtained when Cl⁻ was returned to the apical bath (Fig. 3C). In contrast, when gluconate substitution was followed by SO₄²⁻ (Fig. 3B), the recovery of pH_i was much slower ($-0.025 \pm 0.024 \text{ min}^{-1}$, $n = 7$).

pH_i recovery rates measured with these and other anions are summarized in Fig. 3C. While the monovalent organic anion HCOO⁻ appeared to be as effective as Cl⁻ in supporting exchange with HCO₃⁻, virtually no recovery of pH_i was observed with the divalent organic anion succinate. The selectivity sequence was as follows: Cl⁻ ~ HCOO⁻ > I⁻ >> SO₄²⁻ ~ succinate. This suggests that the cAMP-stimulated anion exchanger at the apical membrane of Calu-3 cells is selective to monovalent anions and, unlike most members of the SLC26 family, does not transport SO₄²⁻.

Inhibitor Sensitivity of Anion Exchange at the Apical Membrane

To further characterize the putative apical anion exchanger, we next examined its inhibitor sensitivity. DIDS at 100 μM, which totally blocked the basolateral exchanger (Fig. 1B), showed only a small inhibitory effect on the apical exchanger (Fig. 2D). Increasing the concentration of DIDS to 500 μM was only slightly more effective (Fig. 4A), suggesting that, whatever the mechanism of apical Cl⁻/HCO₃⁻ exchange, it is quite insensitive to DIDS.

An alternative pathway for anion movements across the apical membrane of cAMP-stimulated cells could be provided by CFTR. We therefore examined the effect of the CFTR channel blocker CFTR_{inh}-172. In cells stimulated with forskolin and IBMX, the addition of CFTR_{inh}-172 (10 μM) to the apical membrane substantially reduced the alkalinization evoked by apical Cl⁻ substitution (Fig. 4B). The effects of different concentrations of DIDS and CFTR_{inh}-172 are summarized in Fig. 4C. The results suggest that the alkalinization resulting from Cl⁻/HCO₃⁻ exchange across the apical membrane is markedly dependent on CFTR and might even occur via the channel itself, rather than an associated anion exchanger.

Unmasking of Basolateral Anion Exchange

Because cAMP stimulation appears to activate Cl⁻/HCO₃⁻ exchange at the apical membrane, it is possible that any alkalinization resulting from Cl⁻ substitution at the basolateral membrane might be masked by HCO₃⁻ efflux at the apical membrane. To test this possibility, we repeated the experiment shown in Fig. 2B in the presence of apical CFTR_{inh}-172 to block apical HCO₃⁻ conductance. Under these conditions, substitution of basolateral Cl⁻ caused a marked alkalinization (Fig. 4D) that was comparable to the response in the unstimulated cells (Fig. 1A). This suggests that stimulation does not inhibit Cl⁻/HCO₃⁻ exchange via AE2 at the basolateral membrane, as previously reported (11, 12). It is, however, consistent with the recent suggestion that the basolateral exchanger

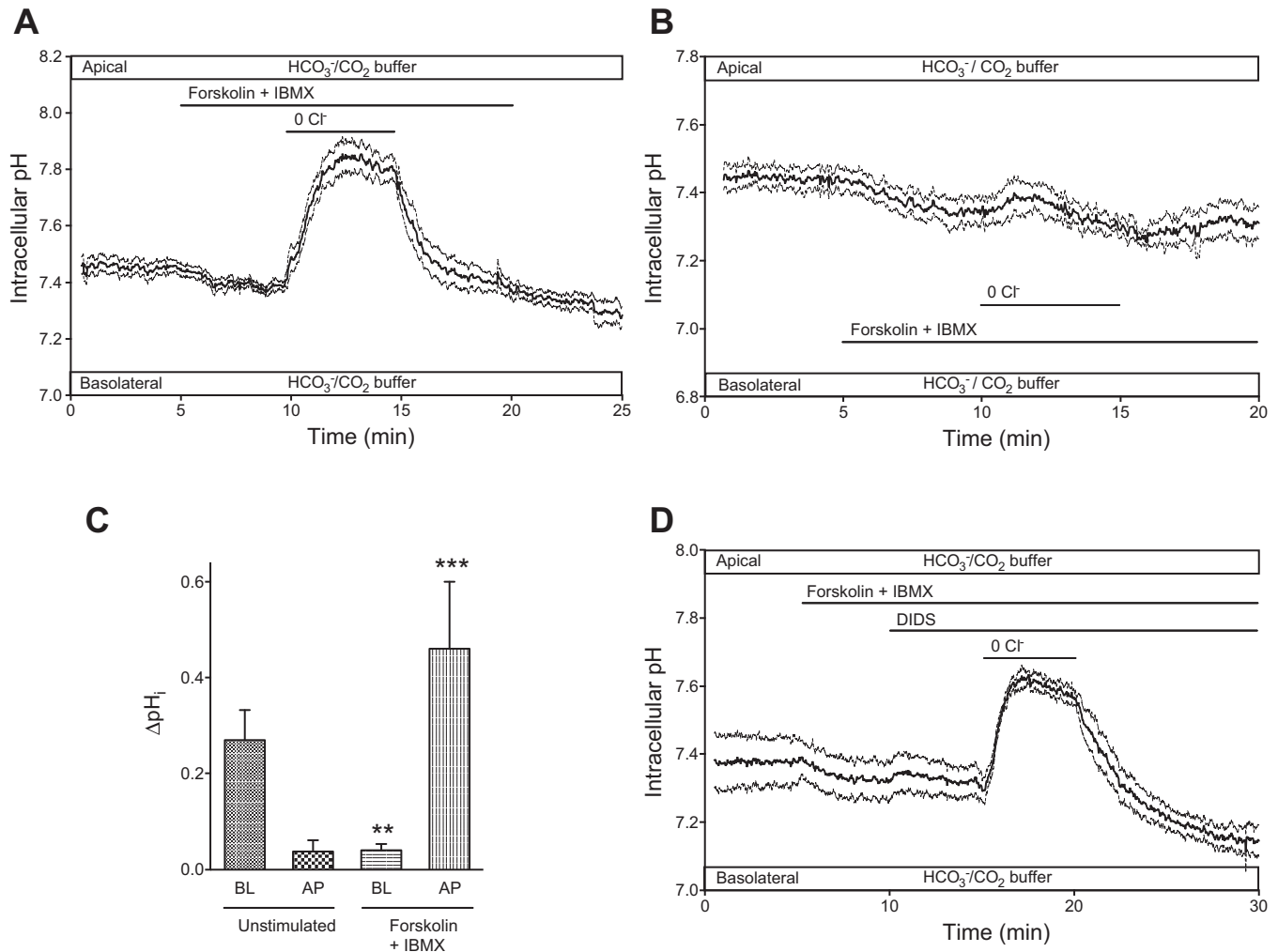


Fig. 2. Effects of apical and basolateral Cl⁻ substitution on p_H_i in cAMP-stimulated Calu-3 cells. Cells were superfused with a HCO₃⁻-buffered solution and stimulated with 10 μM forskolin and 100 μM IBMX. *A*: changes in p_H_i evoked by gluconate substitution of Cl⁻ at the apical membrane (*n* = 9). *B*: effects of basolateral Cl⁻ substitution (*n* = 4). *C*: changes in p_H_i evoked by basolateral (BL) and apical (AP) Cl⁻ substitution in unstimulated and forskolin-stimulated cells. Values are means ± SE. ***P* < 0.01, ****P* < 0.001 compared with unstimulated control (by Student's *t*-test). *D*: lack of effect of DIDS (100 μM) on the response of stimulated cells to apical Cl⁻ substitution (*n* = 4). In *A*, *B*, and *D*, solid lines represent averaged p_H_i time course from *n* identical experiments and dashed lines represent SE.

contributes to Cl⁻ uptake across the basolateral membrane during stimulated secretion (55).

Expression of SLC26 Transporters

RT-PCR was used to assess the expression of a number of SLC26 transporters that might be responsible for Cl⁻/HCO₃⁻ exchange across the apical membrane of Calu-3 cells. Of the 10 members of the SLC26 family, those examined were SLC26A2 (because of its widespread tissue distribution), SLC26A3, SLC26A4, and SLC26A6 (the Cl⁻/HCO₃⁻ exchangers), and SLC26A7 and SLC26A9 (the Cl⁻ channels).

As shown in Fig. 5A, 18S rRNA was used as a positive control and reference. CFTR and AE2, which are expected to be abundant in Calu-3 cells, were readily detected by RT-PCR and appeared as strong bands. All the SLC26 gene family members tested were detectable, and their expected PCR product sizes were confirmed.

The next step was to quantify their mRNA expression relative to other transporters known to be functionally impor-

tant. Using real-time qPCR, the relative mRNA expression levels of the SLC26 family members were compared with CFTR and AE2 after normalization to 18S rRNA.

As shown in Fig. 5B, the qPCR measurements showed only low levels of SLC26 transporter mRNA compared with the much higher levels for CFTR and AE2. Of the SLC26 family members examined, only SLC26A2 and SLC26A6 showed significant levels of mRNA expression at 26.4 ± 7.9% and 11.1 ± 2.6% of the CFTR level, respectively (*n* = 6). SLC26A4 (0.13 ± 0.04%), SLC26A7 (1.5 ± 0.8%), and SLC26A9 (0.08 ± 0.02%) showed very low levels of expression compared with CFTR. The C_T value of SLC26A3 was undetermined in the qPCR analysis, although the SLC26A3 PCR product was just visible as a very faint band on the gel.

Driving Force for Apical Cl⁻ Efflux

For the alkalinization evoked by apical Cl⁻ substitution to be sustained (Fig. 2A), there must be continuous uptake of Cl⁻ across the basolateral membrane. Since this is mediated, at

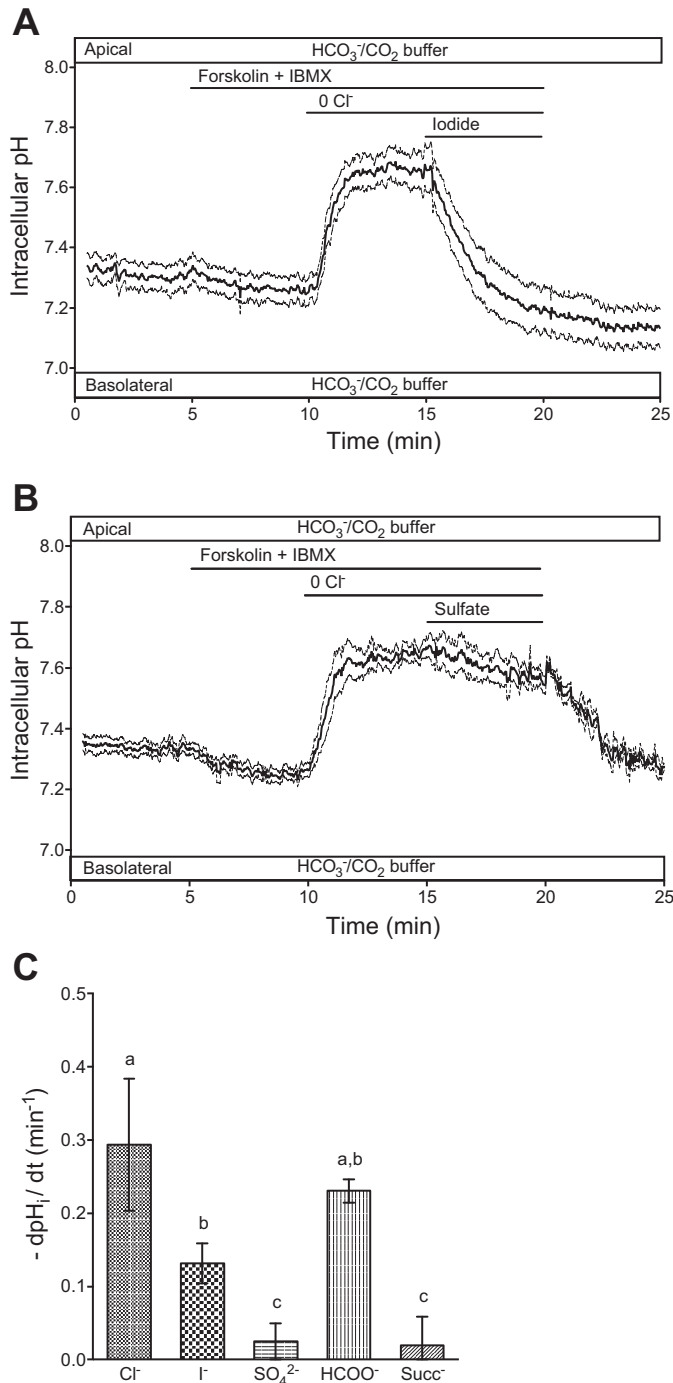


Fig. 3. Anion selectivity of recovery of p_Hi from alkalization induced by substitution of apical Cl⁻. Cells were superfused with a HCO₃⁻-buffered solution and stimulated with 10 μM forskolin and 100 μM IBMX. *A* and *B*: after 5 min of Cl⁻ substitution with gluconate, gluconate was replaced by I⁻ and SO₄²⁻. Solid lines represent averaged p_Hi time course from 6 and 7 experiments, respectively, and dashed lines represent SE. *C*: initial rates of recovery of p_Hi (dp_Hi/dt) when apical gluconate was replaced by Cl⁻, I⁻, SO₄²⁻, HCOO⁻, and succinate (Succ⁻). Values are means ± SE from ≥6 experiments. *a*, *b* and *c* indicate groups identified by post hoc Tukey's test as statistically distinct from each other (*P* < 0.05).

least in part, by the basolateral Na⁺-K⁺-2Cl⁻ cotransporter NKCC1, we examined the effect of applying the NKCC1 inhibitor bumetanide (300 μM) at the basolateral membrane. As shown in Fig. 6*A*, pretreatment with bumetanide halved the initial magnitude of the alkalization (Δp_Hi = 0.18 ± 0.03) compared with Fig. 2*A* (Δp_Hi = 0.46 ± 0.14), and the p_Hi declined slowly during the substitution period.

An additional pathway for Cl⁻ uptake across the basolateral membrane is provided by the AE2 Cl⁻/HCO₃⁻ exchanger working in parallel with the transporters that accumulate intracellular HCO₃⁻, namely, NBC1 and NHE1. Since AE2 is inhibited by 100 μM DIDS, this was applied, in combination with bumetanide, to block both uptake pathways in the experiment shown in Fig. 6*B*. Although an initial alkalization was observed, it was transient and vanished in <5 min. The most straightforward interpretation of these results is that Cl⁻ uptake across the basolateral membrane via NKCC1, and especially AE2, is vital for sustaining the alkalization observed during apical Cl⁻ substitution.

Driving Force for Apical HCO₃⁻ Influx

In forskolin-stimulated cells, CFTR provides a major pathway for Cl⁻ efflux across the apical membrane. How could CFTR alone mediate what appears to be Cl⁻/HCO₃⁻ exchange at the apical membrane? After gluconate substitution of apical Cl⁻, rapid Cl⁻ efflux will inevitably depolarize the apical membrane, and this depolarization could, if large enough, reverse the normally outwardly directed electrochemical gradient for HCO₃⁻. Given that CFTR is also permeable to HCO₃⁻, this could result in simultaneous entry of HCO₃⁻ and efflux of Cl⁻ via CFTR, and this might account for the alkalization and its sensitivity to CFTR_{inh-172}.

To test the feasibility of this hypothetical mechanism, we examined the effect of hyperpolarizing the cells by applying the K⁺ channel opener 5,6-dichloro-1-ethyl-1,3-dihydro-2H-benzimidazol-2-one (DCEBIO; 10 μM) on the basolateral side (6). As shown in Fig. 6*C*, although the initial alkalization response to apical Cl⁻ removal was similar to that observed under control conditions (Fig. 2*A*), it was not sustained. This suggests that the driving force for HCO₃⁻ entry across the apical membrane had been reduced, which is what we would expect if the depolarizing effect of Cl⁻ efflux had been counteracted by the hyperpolarizing effect of DCEBIO.

To estimate the magnitude of the depolarization that was induced by substituting Cl⁻ in the bath, we used the perforated-patch technique to measure the associated membrane potential changes in Calu-3 cells freshly isolated from fully differentiated, polarized monolayers. The resting potential of cells bathed in the HEPES-buffered solution was -28.7 ± 10.0 mV (*n* = 12). When the Cl⁻ in the bathing medium was replaced with gluconate during forskolin stimulation (Fig. 7*A*), the membrane potential depolarized rapidly, presumably as a result of Cl⁻ efflux via CFTR, and reversed to +28.0 ± 19.8 mV (*n* = 6, *P* < 0.05). It then repolarized slowly, probably as a result of the gradual depletion of intracellular Cl⁻, since these isolated cells were completely bathed in the Cl⁻-free solution.

In cells bathed with the HCO₃⁻-buffered solution, the resting membrane potential (-25.4 ± 7.3 mV, *n* = 12) was not significantly different from that in cells bathed with the

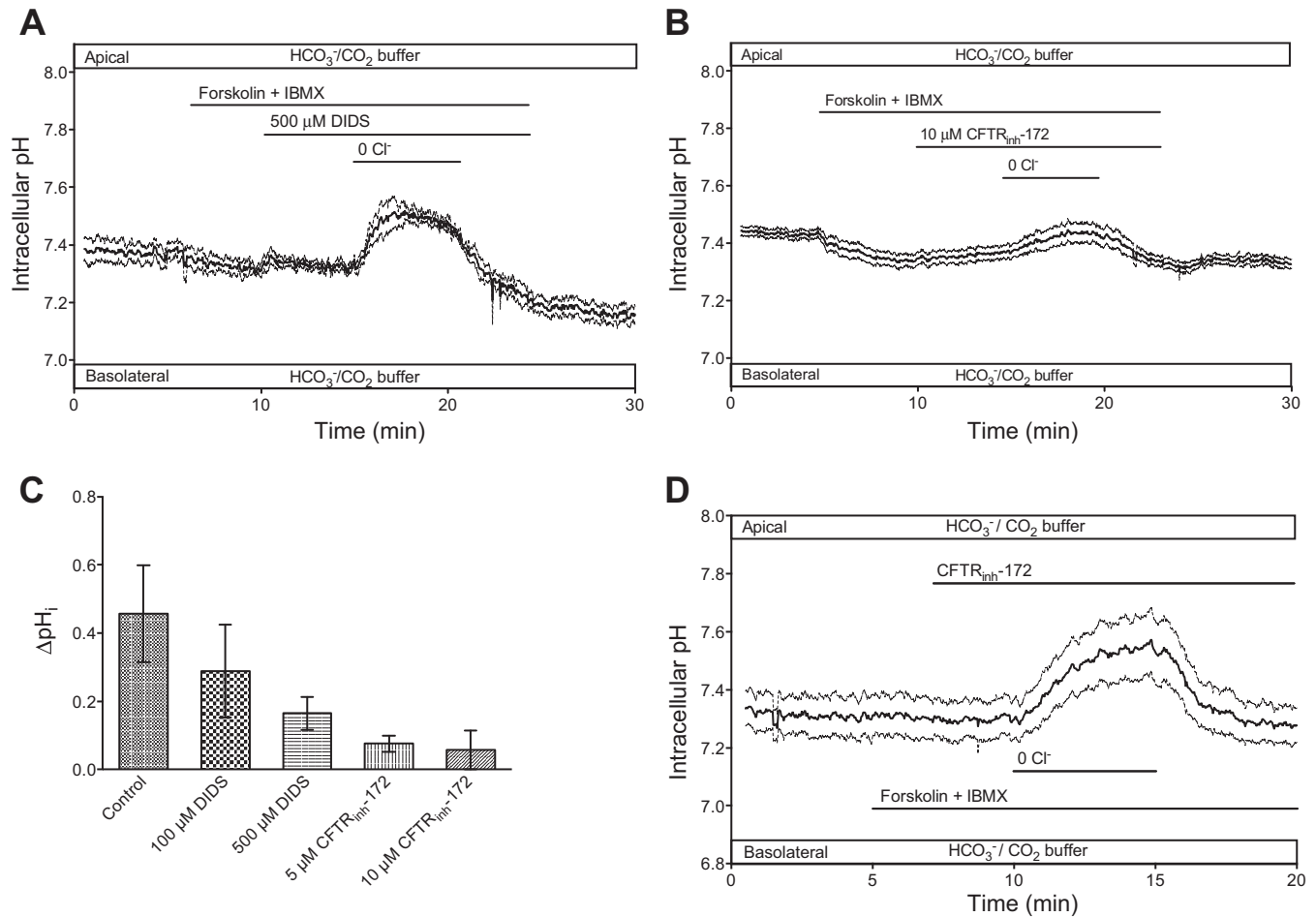


Fig. 4. Effects of DIDS and CFTR_{inh}-172 on pH_i changes evoked by apical Cl⁻ substitution in cAMP-stimulated Calu-3 cells. Cells were superfused with a HCO₃⁻-buffered solution and stimulated with 10 μM forskolin and 100 μM IBMX. *A*: changes in pH_i evoked by gluconate substitution of Cl⁻ at the apical membrane in the presence of 500 μM DIDS (*n* = 4). *B*: effects of apical Cl⁻ substitution in the presence of 10 μM CFTR_{inh}-172 (*n* = 4). *C*: effects of different concentrations of DIDS and CFTR_{inh}-172 on pH_i changes evoked by apical Cl⁻ substitution. Values are means ± SE. All are significantly different from control (*P* < 0.05, by Student's unpaired *t*-test). *D*: effect of apical CFTR_{inh}-172 (10 μM) on pH_i changes evoked by basolateral Cl⁻ substitution in forskolin-stimulated cells (*n* = 5). In *A*, *B*, and *D*, solid lines represent averaged pH_i time course from *n* identical experiments and dashed lines represent SE.

HEPES-buffered solution. Stimulation with forskolin and IBMX caused a transient hyperpolarization (Fig. 7*B*), which could be due to electrogenic HCO₃⁻ uptake via NBC1, as previously observed in pancreatic duct cells (24). Substitution of extracellular Cl⁻ with gluconate again caused a rapid depolarization and reversal to a positive membrane potential (+21.6 ± 8.7 mV, *n* = 4, *P* < 0.01). After partial repolarization, membrane potential remained markedly depolarized (+13.6 ± 7.4 mV after 2 min) before returning to its initial value when Cl⁻ was restored to the bath. When these experiments were repeated in the presence of 10 μM CFTR_{inh}-172, the voltage change induced by Cl⁻ substitution was greatly reduced, and there was no reversal of the membrane potential (Fig. 7*C*). This indicates that the changes in membrane potential evoked by Cl⁻ substitution were due to Cl⁻ efflux via CFTR, rather than another electrogenic pathway.

The key finding here is that, during Cl⁻ substitution, the membrane potential increased sufficiently to reverse the electrochemical gradient for HCO₃⁻ and, therefore, would drive HCO₃⁻ entry through CFTR channels. HCO₃⁻ entry by this mechanism, which was not excluded in previous studies, could

explain the intracellular alkalinization evoked by apical Cl⁻ substitution in polarized Calu-3 monolayers. It would also account for the acute sensitivity of the intracellular alkalinization to CFTR_{inh}-172 and the fact that we have been unable to detect significant AE or SLC26 activity at the apical membrane.

DISCUSSION

A standard experimental approach for detecting Cl⁻/HCO₃⁻ exchange across cell membranes is to substitute extracellular Cl⁻ with a nontransported anion, such as gluconate, and to record the resulting change in pH_i. This method has been used to characterize anion exchangers in a wide range of polarized and unpolarized cells (2, 56, 58, 61). The assumption is that if a Cl⁻/HCO₃⁻ exchanger is present, sudden reversal of the Cl⁻ gradient will drive intracellular Cl⁻ out of the cell in exchange for extracellular HCO₃⁻, and the resulting entry of HCO₃⁻ will cause a rise in pH_i. However, the same phenomenon can arise as a result of electrically coupled Cl⁻ and HCO₃⁻ movements through an anion chan-

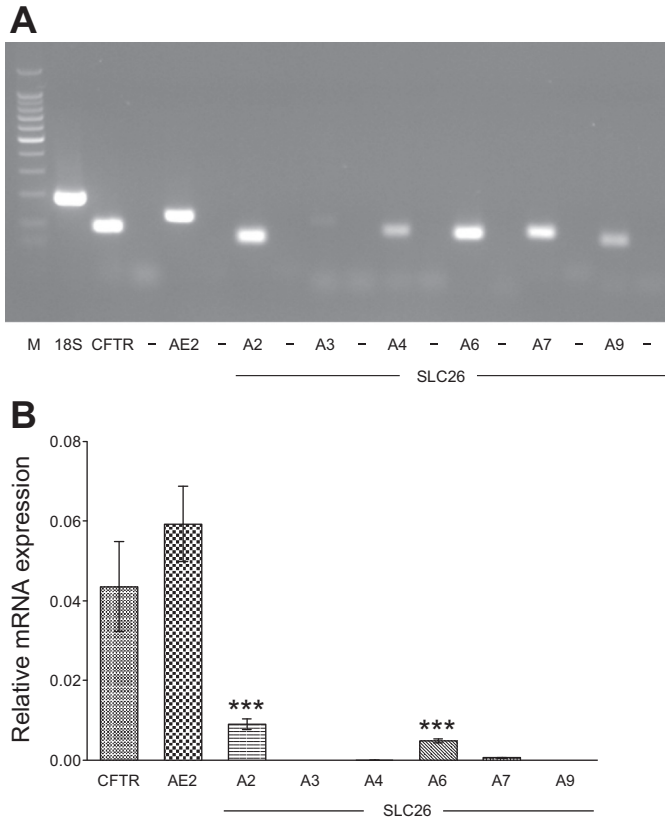


Fig. 5. mRNA expression of anion transporters in polarized Calu-3 cells assessed by quantitative RT-PCR. *A*: agarose gel showing products of conventional RT-PCR using the primers listed in Table 1. 18S rRNA was used as the endogenous control gene reference, and the strong single band indicates that the cDNA was of good quality. RT-negative control lanes (–), omitting the RT step, confirm the absence of contamination. *B*: quantitative PCR measurements of mRNA expression normalized to 18S rRNA. Relative mRNA expression was calculated by the cycle threshold ($2^{-\Delta\Delta C_T}$) method (33). Values are means \pm SE from 6 experiments. Analysis of variance indicated that mRNA expression levels of each of the solute carrier family 26 (SLC26) transporters (A2, A3, A4, A6, A7, and A9) differed significantly from CFTR and anion exchanger 2 (AE2) ($P < 0.001$) and that SLC26A2 and SLC26A6 transcripts were present at significantly higher levels than the other SLC26 transporters. *** $P < 0.001$.

nel such as CFTR, and this possibility was not excluded in previous studies of Calu-3 cells (11, 12).

At first sight, the Cl^- substitution data presented here suggest that unstimulated Calu-3 cells show $\text{Cl}^-/\text{HCO}_3^-$ exchange at the basolateral membrane, but not at the apical membrane. After forskolin stimulation, $\text{Cl}^-/\text{HCO}_3^-$ exchange at the basolateral membrane disappeared, and brisk $\text{Cl}^-/\text{HCO}_3^-$ exchange became evident at the apical membrane. The simplest interpretation of these data is that elevated cAMP inhibits the basolateral exchanger, known to be AE2 (34), and activates a different exchanger, possibly a member of the SLC26 family, at the apical membrane. Indeed, this was our conclusion when we first reported our preliminary results (35). It is also the conclusion of a more recent study by Garnett et al. (11). Similar to our findings, Garnett et al. attributed the apical $\text{Cl}^-/\text{HCO}_3^-$ exchange in cAMP-stimulated Calu-3 cells to the SLC26 transporter pendrin (SLC26A4). This was based mainly on its selectivity to monovalent anions and its insensitivity to inhibition by DIDS.

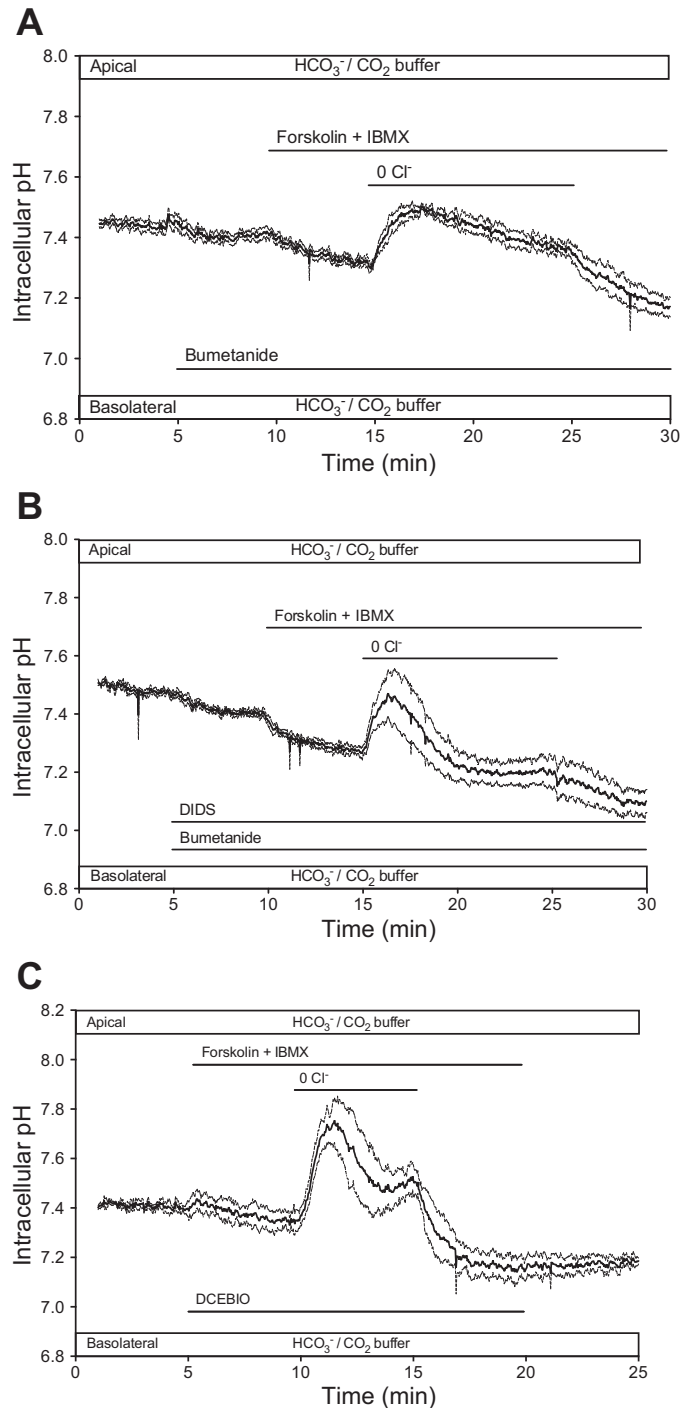


Fig. 6. Alkalinization evoked by apical Cl^- substitution in forskolin-stimulated Calu-3 cells is dependent on basolateral Cl^- uptake and membrane potential. Cells were superfused with the HCO_3^- -buffered solution, stimulated with forskolin and IBMX, and exposed to a Cl^- -free solution at the apical surface. *A*: effect of pretreatment with bumetanide (300 μM) to inhibit the basolateral $\text{Na}^+/\text{K}^+/\text{2Cl}^-$ cotransporter 1 (NKCC1; $n = 5$). *B*: effect of pretreatment with DIDS (100 μM), in addition to bumetanide, to inhibit basolateral AE2 and NKCC1 ($n = 5$). *C*: effect of the K^+ channel opener 5,6-dichloro-1-ethyl-1,3-dihydro-2H-benzimidazol-2-one (DCEBIO, 10 μM) to hyperpolarize the cells ($n = 4$). Solid lines represent averaged pH_i time course from n identical experiments, and dashed lines represent SE.

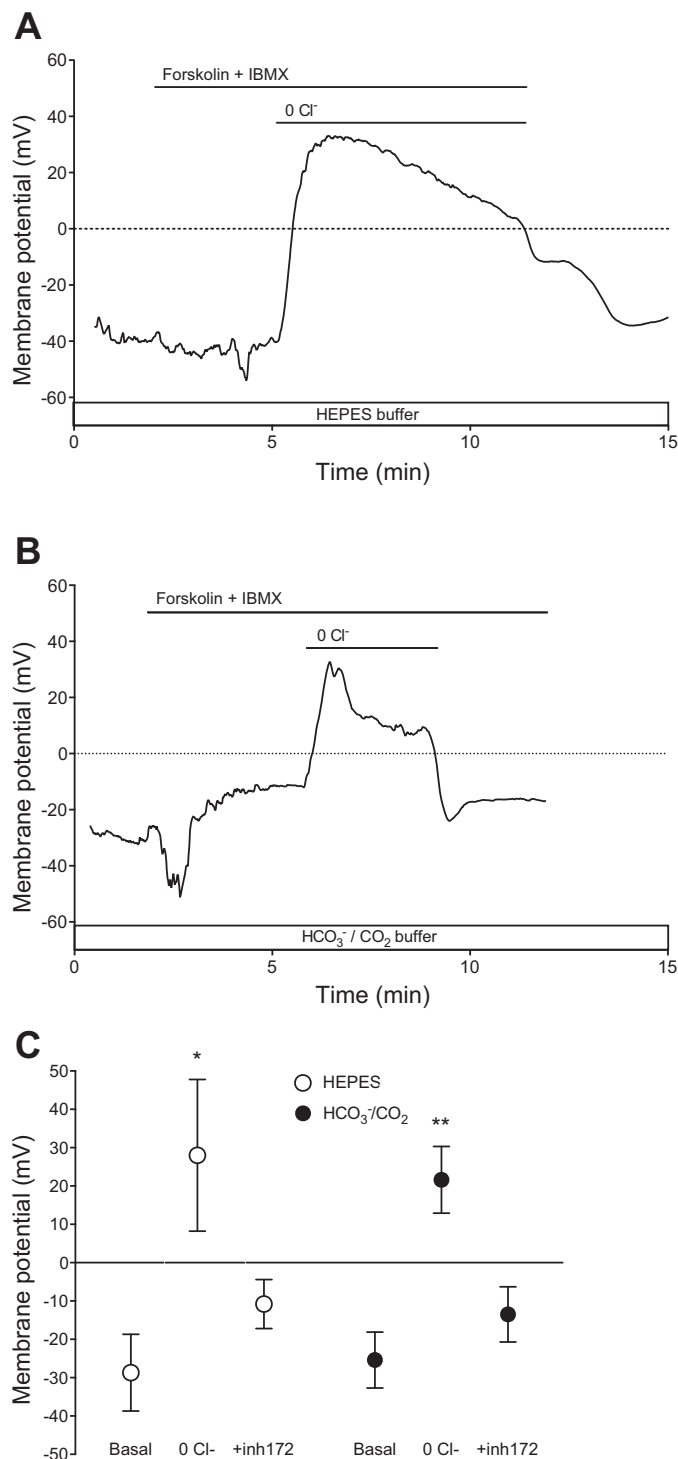


Fig. 7. Perforated-patch measurements of membrane potential changes evoked by Cl^- substitution in isolated Calu-3 cells. Cells were superfused with HEPES-buffered (A) or HCO_3^- -buffered (B) solution at room temperature. Forskolin (10 μM) and IBMX (100 μM) were added, and Cl^- was substituted with gluconate. C: summary of membrane potentials (means \pm SE) recorded before (basal) and after Cl^- substitution (0 Cl^-) in the absence ($n = 5$) or presence ($n = 4$) of HCO_3^- . Also shown are membrane potentials recorded after Cl^- substitution, when cells were pretreated with 10 μM CFTR_{inh}-172 (+inh172, $n = 3$ in both cases). * $P < 0.05$, ** $P < 0.01$ compared with corresponding basal value (by ANOVA).

However, the pendrin hypothesis raises a number of concerns, which have led us to reconsider our interpretation. First, a substantial body of evidence in the existing literature, mainly from Ussing chamber studies, indicates that apical HCO_3^- secretion is mediated mainly by CFTR and that these cells have no requirement for an apical anion exchanger (6, 18, 20, 29, 30). Indeed, under pH-stat conditions the HCO_3^- secretion by Calu-3 cells is slightly higher in bilateral Cl^- -free gluconate than normal extracellular Cl^- solution, which is not compatible with HCO_3^- exit by obligatory anion exchange (55). Second, our own studies suggest that 1) pendrin expression is very low in Calu-3 cells, 2) the characteristics of apical anion exchange are more consistent with the properties of CFTR, and 3) electrochemical gradients sufficient to drive conductive, CFTR-mediated Cl^- efflux and HCO_3^- uptake can be induced under conditions that are commonly used to study anion exchange (27).

Is Apical HCO_3^- Transport Mediated by Pendrin or CFTR?

SLC26 expression levels. Although mRNAs for several members of the SLC26 family were detectable in the Calu-3 monolayers by RT-PCR, the mRNA expression levels measured by qPCR were much lower for the SLC26 transporters than for CFTR and AE2. In particular, pendrin mRNA was present at $<0.2\%$ of the CFTR transcript level. The only mRNAs present to any significant degree were for SLC26A2, which is a SO_4^{2-} transporter that does not mediate $\text{Cl}^- / \text{HCO}_3^-$ exchange (40), and for SLC26A6, which is DIDS-sensitive and accepts divalent anions (1). While the low level of pendrin mRNA does not preclude some protein expression, we were unable to find evidence for this when we probed immunoblots of Calu-3 cell lysates with five different pendrin antibodies (data not shown). It is interesting to note that Garnett et al. (11) could only detect sparse labeling for pendrin in Calu-3 monolayers, whereas intense labeling is observed at the apical membrane of human tracheal and bronchial surface epithelium (37, 41).

Inhibitor sensitivity. While the insensitivity of apical $\text{Cl}^- / \text{HCO}_3^-$ exchange to DIDS inhibition would be consistent with the known properties of pendrin (48), its marked sensitivity to CFTR_{inh}-172 is more difficult to explain. CFTR is known to activate SLC26 transporters through protein-protein interactions (28), but, as far as we are aware, there is no evidence to suggest that blocking the CFTR channel reduces this stimulatory effect. Garnett et al. (11) also reported that apical $\text{Cl}^- / \text{HCO}_3^-$ exchange was abolished by CFTR blockers. However, they provided evidence to suggest that apical $\text{Cl}^- / \text{HCO}_3^-$ exchange persisted after CFTR_{inh}-172 but was not detected due to basolateral AE2 activity, which would reduce intracellular accumulation of HCO_3^- . This may be true, although it is difficult to reconcile with their claim that the basolateral AE2 is inhibited in cAMP-stimulated cells. Alternatively, the residual fluxes they report may reflect incomplete inhibition of CFTR by the CFTR blockers, and the small inhibitory effect of high concentrations of DIDS that we observed could be due to the weak, but significant, effect of DIDS on CFTR (47). Either way, it is difficult to escape the conclusion that most of the Cl^- and HCO_3^- fluxes are mediated directly by CFTR, rather than by an anion exchanger such as pendrin.

Anion selectivity. Our anion selectivity data suggest that the transporter responsible for experimentally induced apical $\text{Cl}^-/\text{HCO}_3^-$ exchange accepts a number of monovalent anions, including HCOO^- , but is unable to transport the divalent anions SO_4^{2-} and succinate. Superficially, this would be consistent with the selectivity profiles of both pendrin (51, 52) and CFTR (19). However, the two transporters differ significantly in their relative permeabilities to Cl^- and I^- : pendrin preferentially transports I^- over Cl^- ($\text{I}^-/\text{Cl}^- \sim 2$) (51), whereas CFTR is more permeable to Cl^- ($\text{I}^-/\text{Cl}^- \sim 0.6$) (19). In Cl^- substitution experiments on stimulated Calu-3 cells, Garnett et al. (11) obtained an intermediate ratio of ~ 1.3 for the apical exchanger (increasing to ~ 2.1 when CFTR expression was knocked down), indicating the possible involvement of both pendrin and CFTR. In contrast, we estimated the I^- -to- Cl^- ratio to be ~ 0.5 , which would be more consistent with $\text{Cl}^-/\text{HCO}_3^-$ exchange occurring mainly via CFTR.

The relative permeability to HCOO^- estimated from our pH_i data ($\text{HCOO}^-/\text{Cl}^- \sim 0.8$; Fig. 3C) is somewhat higher than the values reported for CFTR in electrophysiological studies (~ 0.4) (19, 32). However, it is likely that our value is overestimated as a consequence of the intracellular acidification resulting from uncharged formic acid entry across the apical membrane.

Driving forces for Cl^- and HCO_3^- fluxes. If we postulate that the apical movements of Cl^- and HCO_3^- in stimulated Calu-3 cells are mediated mainly by CFTR, rather than by an electro-neutral anion exchanger such as pendrin, we can make two predictions. 1) We would expect the alkalinization that follows apical Cl^- substitution to be altered by experimental manipulation of the membrane potential. In support of this, we observed that the alkalinizing influx of HCO_3^- was reduced when the cells were hyperpolarized by exposure to the K^+ channel opener DCEBIO (Fig. 6C). 2) We have calculated the apical membrane potential that would be required to reverse the normally outward flux of HCO_3^- through CFTR. During apical Cl^- substitution, pH_i rises to ~ 7.8 , which corresponds to an intracellular HCO_3^- concentration of ~ 60 mM, compared with 25 mM in the apical bathing solution. A reversal of the apical membrane potential to at least +23 mV would be required for HCO_3^- to enter the cell against this concentration gradient. Although we were unable to measure membrane potential in polarized Calu-3 monolayers, we were able to do so using the perforated-patch technique to record from single cells that had been freshly isolated from monolayers. In these experiments, substituting extracellular Cl^- caused the intracellular potential to rise to more than +20 mV (Fig. 7). Given that basolateral Cl^- uptake, which is necessary for sustained depolarization of the apical membrane, was also unavoidably blocked in these experiments, the membrane potential change was probably underestimated. These data are therefore consistent with HCO_3^- entering the cells mainly via CFTR during extracellular Cl^- substitution.

Although the resting intracellular potential in freshly isolated Calu-3 cells was ~ 20 mV more positive than the apical membrane potential reported previously in confluent Calu-3 monolayers using microelectrodes (62), the values in forskolin-stimulated cells were very similar, despite the different experimental conditions (62). More importantly, however, the impact of extracellular Cl^- substitution on intracellular potential would have been blunted in our perforated-patch recordings by

the presence of basolateral membrane conductances, which are essentially in parallel with CFTR under these conditions. In other words, the changes in apical membrane potential evoked by Cl^- substitution would almost certainly have been underestimated compared with confluent monolayers where apical membrane potential is dominated by the anion-selective conductance of CFTR channels (62). Thus we predict that an even more positive voltage would be observed during apical Cl^- substitution in confluent monolayers, further strengthening the conclusion that Cl^- efflux through CFTR can drive conductive HCO_3^- uptake and intracellular alkalinization.

While we cannot exclude a small contribution from pendrin, and perhaps also from SLC26A6 given the significant expression of its transcript, we conclude that the observed apical fluxes of Cl^- and HCO_3^- evoked by Cl^- substitution are most likely mediated mainly by CFTR in Calu-3 cells. This would certainly be more consistent with previous work on these cells (6, 18, 20, 29, 30), including recent pH-stat studies of HCO_3^- secretion in cells bathed in Cl^- -free medium (55). It is interesting to note that, in another HCO_3^- -secreting epithelium, the parotid duct, pendrin contributes to the secretion of I^- , but not HCO_3^- , the latter of which is transported mainly via SLC26A6 (56). In human airway surface epithelium, where pendrin is undoubtedly expressed at the apical membrane and is dramatically induced by proinflammatory cytokines, it is thought to be primarily involved in antimicrobial SCN^- secretion (41) and in regulation of mucus secretion (37).

A commonly perceived problem with a secretory model in which CFTR is the sole pathway for both Cl^- and HCO_3^- efflux is that CFTR has a much lower permeability to HCO_3^- ($P_{\text{HCO}_3^-}$) than to Cl^- (P_{Cl^-}). Values for $P_{\text{HCO}_3^-}/P_{\text{Cl}^-}$ in the literature range from 0.13 to 0.25 (19, 32, 39, 43). Consequently, an alternative model in which fluid secretion is driven by Cl^- transport via CFTR and most of the HCO_3^- content arises through secondary $\text{Cl}^-/\text{HCO}_3^-$ exchange via pendrin (11) is superficially more attractive. However, as demonstrated previously, even if $P_{\text{HCO}_3^-}/P_{\text{Cl}^-}$ is low, a secretion rich in HCO_3^- can be generated via CFTR alone if the electrochemical gradient for Cl^- is significantly smaller than that for HCO_3^- (6, 23).

Role of Basolateral AE2 in Cl^- and HCO_3^- Secretion

AE2 is ubiquitously expressed at the basolateral membrane of secretory epithelial cells (49), and its presence in Calu-3 cells is well documented (16, 34). While it has an important role protecting cells from intracellular alkalinization, it can also be involved in cell volume regulation and transepithelial Cl^- secretion. Working in parallel with NHE1 or NBC1, it provides an electrically silent pathway for Cl^- uptake against an opposing electrochemical gradient (13, 38, 65). For an epithelium striving to generate HCO_3^- -rich secretions, however, the activity of AE2 has two adverse effects: 1) it provides a "leak" for intracellular HCO_3^- back to the basal interstitium, and 2) it contributes to the driving force for apical Cl^- secretion, making secretion of high HCO_3^- concentrations more difficult. This is a serious issue for epithelia such as the guinea pig pancreatic duct, which can secrete 140 mM HCO_3^- , and there is evidence to suggest that this requires suppression of AE2 activity (22).

At first sight, the same appears to be occurring in Calu-3 cells. The alkalinization that results from basolateral Cl^-

substitution is almost totally abolished during forskolin stimulation (Fig. 2D), suggesting that AE2 activity is somehow suppressed. Others have proposed that this may be due to an unidentified protein kinase (12); however, the results in Fig. 4D suggest an alternative explanation. The fact that apical application of CFTR_{inh}-172 restores the alkalization indicates that AE2 remains active in the stimulated cells and that CFTR prevents the increase in pH by allowing a compensatory efflux of HCO₃⁻ at the apical membrane.

This alternative interpretation is consistent with recent work suggesting that Cl⁻ uptake via AE2, rather than via NKCC1, provides the main driving force for Cl⁻ secretion in Calu-3 cells (16) and accounts for its marked dependence on HCO₃⁻ (55). In any case, since Calu-3 cells secrete only moderate concentrations of HCO₃⁻, there is probably no requirement for suppression of basolateral Cl⁻ uptake during stimulation.

In summary, and contrary to our initial interpretation of the Cl⁻ substitution data, we believe that HCO₃⁻ transport across the apical membrane of stimulated Calu-3 cells, during apical Cl⁻ substitution and also during normal secretion, is mediated mainly by CFTR, rather than by a separate anion exchanger. In addition, our data suggest that basolateral AE2 activity is not suppressed during cAMP stimulation and that it may therefore make a significant contribution to transepithelial Cl⁻ secretion through the HCO₃⁻-dependent uptake of Cl⁻ across the basolateral membrane.

ACKNOWLEDGMENTS

We thank Prof. John Hanrahan (McGill University, Montreal, PQ, Canada) for helpful discussions.

GRANTS

D. Kim was supported by an Overseas Research Students Award from the University of Manchester. B. Burghardt was supported by an International Incoming Short Visit Award from the Royal Society.

DISCLOSURES

No conflicts of interest, financial or otherwise, are declared by the authors.

AUTHOR CONTRIBUTIONS

D.K., J.K., B.B., L.B., and M.C.S. are responsible for conception and design of the research; D.K. and J.K. performed the experiments; D.K., J.K., B.B., L.B., and M.C.S. analyzed the data; D.K., J.K., B.B., L.B., and M.C.S. interpreted the results of the experiments; D.K. and M.C.S. prepared the figures; D.K. and M.C.S. drafted the manuscript; D.K. and M.C.S. edited and revised the manuscript; M.C.S. approved the final version of the manuscript.

REFERENCES

- Alper SL, Sharma AK. The SLC26 gene family of anion transporters and channels. *Mol Aspects Med* 34: 494–515, 2013.
- Amlal H, Petrovic S, Xu J, Wang ZH, Sun XM, Barone S, Soleimani M. Deletion of the anion exchanger Slc26a4 (pendrin) decreases apical Cl⁻/HCO₃⁻ exchanger activity and impairs bicarbonate secretion in kidney collecting duct. *Am J Physiol Cell Physiol* 299: C33–C41, 2010.
- Boucher RC. Cystic fibrosis: a disease of vulnerability to airway surface dehydration. *Trends Mol Med* 13: 231–240, 2007.
- Boucher RC. Molecular insights into the physiology of the “thin film” of airway surface liquid. *J Physiol* 516: 631–638, 1999.
- Coakley RD, Grubb BR, Paradiso AM, Gatzky JT, Johnson LG, Kreda SM, O’Neal WK, Boucher RC. Abnormal surface liquid pH regulation by cultured cystic fibrosis bronchial epithelium. *Proc Natl Acad Sci USA* 100: 16083–16088, 2003.
- Devor DC, Singh AK, Lambert LC, DeLuca A, Frizzell RA, Bridges RJ. Bicarbonate and chloride secretion in Calu-3 human airway epithelial cells. *J Gen Physiol* 113: 743–760, 1999.
- Dorwart MR, Shcheynikov N, Yang DK, Muallem S. The solute carrier 26 family of proteins in epithelial ion transport. *Physiology* 23: 104–114, 2008.
- Engelhardt JF, Yankaskas JR, Ernst SA, Yang YP, Marino CR, Boucher RC, Cohn JA, Wilson JM. Submucosal glands are the predominant site of CFTR expression in the human bronchus. *Nat Genet* 2: 240–248, 1992.
- Fahy JV, Dickey BF. Airway mucus function and dysfunction. *N Engl J Med* 363: 2233–2247, 2010.
- Fischer H, Widdicombe JH. Mechanisms of acid and base secretion by the airway epithelium. *J Membr Biol* 211: 139–150, 2006.
- Garnett JP, Hickman E, Burrows R, Hegyi P, Tislavicz L, Cuthbert AW, Fong P, Gray MA. Novel role for pendrin in orchestrating bicarbonate secretion in cystic fibrosis transmembrane conductance regulator (CFTR)-expressing airway serous cells. *J Biol Chem* 286: 41069–41082, 2011.
- Garnett JP, Hickman E, Tunkammerthai O, Cuthbert AW, Gray MA. Protein phosphatase 1 coordinates CFTR-dependent airway epithelial HCO₃⁻ secretion by reciprocal regulation of apical and basolateral membrane Cl⁻-HCO₃⁻ exchangers. *Br J Pharmacol* 168: 1946–1960, 2013.
- Gawenis LR, Bradford EM, Alper SL, Prasad V, Shull GE. AE2 Cl⁻/HCO₃⁻ exchanger is required for normal cAMP-stimulated anion secretion in murine proximal colon. *Am J Physiol Gastrointest Liver Physiol* 298: G493–G503, 2010.
- Gustafsson JK, Ermund A, Ambort D, Johansson MEV, Nilsson HE, Thorell K, Hebert H, Sjoval H, Hansson GC. Bicarbonate and functional CFTR channel are required for proper mucin secretion and link cystic fibrosis with its mucus phenotype. *J Exp Med* 209: 1263–1272, 2012.
- Haws C, Finkbeiner WE, Widdicombe JH, Wine JJ. CFTR in Calu-3 human airway cells: channel properties and role in cAMP-activated Cl⁻ conductance. *Am J Physiol Lung Cell Mol Physiol* 266: L502–L512, 1994.
- Huang J, Shan J, Kim D, Liao J, Evagelidis A, Alper SL, Hanrahan JW. Basolateral chloride loading by the anion exchanger type 2: role in fluid secretion by the human airway epithelial cell line Calu-3. *J Physiol* 590: 5299–5316, 2012.
- Hug MJ, Bridges RJ. pH regulation and bicarbonate transport of isolated porcine submucosal glands. *JOP* 2 Suppl 4: 274–279, 2001.
- Hug MJ, Tamada T, Bridges RJ. CFTR and bicarbonate secretion to epithelial cells. *News Physiol Sci* 18: 38–42, 2003.
- Illek B, Tam AW, Fischer H, Machen TE. Anion selectivity of apical membrane conductance of Calu 3 human airway epithelium. *Pflügers Arch* 437: 812–822, 1999.
- Illek B, Yankaskas JR, Machen TE. cAMP and genistein stimulate HCO₃⁻ conductance through CFTR in human airway epithelia. *Am J Physiol Lung Cell Mol Physiol* 272: L752–L761, 1997.
- Irokawa T, Krouse ME, Joo NS, Wu JV, Wine JJ. A “virtual gland” method for quantifying epithelial fluid secretion. *Am J Physiol Lung Cell Mol Physiol* 287: L784–L793, 2004.
- Ishiguro H, Naruse S, Kitagawa M, Mabuchi T, Kondo T, Hayakawa T, Case RM, Steward MC. Chloride transport in microperfused interlobular ducts isolated from guinea-pig pancreas. *J Physiol* 539: 175–189, 2002.
- Ishiguro H, Steward MC, Naruse S, Ko SB, Goto H, Case RM, Kondo T, Yamamoto A. CFTR functions as a bicarbonate channel in pancreatic duct cells. *J Gen Physiol* 133: 315–326, 2009.
- Ishiguro H, Steward MC, Sohma Y, Kubota T, Kitagawa M, Kondo T, Case RM, Hayakawa T, Naruse S. Membrane potential and bicarbonate secretion in isolated interlobular ducts from guinea-pig pancreas. *J Gen Physiol* 120: 617–628, 2002.
- Jacquot J, Puchelle E, Hinnrasky J, Fuchey C, Bettinger C, Spilmont C, Bonnet N, Dieterle A, Dreyer D, Pavirani A, Dalemans W. Localization of the cystic fibrosis transmembrane conductance regulator in airway secretory glands. *Eur Respir J* 6: 169–176, 1993.
- Jiang C, Finkbeiner WE, Widdicombe JH, Miller SS. Fluid transport across cultures of human tracheal glands is altered in cystic fibrosis. *J Physiol* 501: 637–647, 1997.
- Kim D, Steward MC. The role of CFTR in bicarbonate secretion by pancreatic duct and airway epithelia. *J Med Invest* 56 Suppl: 336–342, 2009.
- Ko SB, Zeng WZ, Dorwart MR, Luo X, Kim KH, Millen L, Goto H, Naruse S, Soyombo A, Thomas PJ, Muallem S. Gating of CFTR by the STAS domain of SLC26 transporters. *Nat Cell Biol* 6: 343–350, 2004.

29. Krouse ME, Talbott JF, Lee MM, Joo NS, Wine JJ. Acid and base secretion in the Calu-3 model of human serous cells. *Am J Physiol Lung Cell Mol Physiol* 287: L1274–L1283, 2004.
30. Lee MC, Penland CM, Widdicombe JH, Wine JJ. Evidence that Calu-3 human airway cells secrete bicarbonate. *Am J Physiol Lung Cell Mol Physiol* 274: L450–L453, 1998.
31. Lee MG, Ohana E, Park HW, Yang D, Muallem S. Molecular mechanism of pancreatic and salivary gland fluid and HCO_3^- secretion. *Physiol Rev* 92: 39–74, 2012.
32. Linsdell P, Tabcharani JA, Rommens JM, Hou YX, Chang XB, Tsui LC, Riordan JR, Hanrahan JW. Permeability of wild-type and mutant cystic fibrosis transmembrane conductance regulator chloride channels to polyatomic anions. *J Gen Physiol* 110: 355–364, 1997.
33. Livak KJ, Schmittgen TD. Analysis of relative gene expression data using real-time quantitative PCR and the $2^{-\Delta\Delta C_T}$ method. *Methods* 25: 402–408, 2001.
34. Loffing J, Moyer BD, Reynolds D, Shmukler BE, Alper SL, Stanton BA. Functional and molecular characterization of an anion exchanger in airway serous epithelial cells. *Am J Physiol Cell Physiol* 279: C1016–C1023, 2000.
35. Moore HE, Burghardt B, Steward MC. SLC26 anion exchanger activity in the airway epithelial cell line Calu-3. *J Physiol* 567P: C116, 2005.
36. Mount DB, Romero MF. The SLC26 gene family of multifunctional anion exchangers. *Pflügers Arch* 447: 710–721, 2004.
37. Nakao I, Kanaji S, Ohta S, Matsushita H, Arima K, Yuyama N, Yamaya M, Nakayama K, Kubo H, Watanabe M, Sagara H, Sugiyama K, Tanaka H, Toda S, Hayashi H, Inoue H, Hoshino T, Shiraki A, Inoue M, Suzuki K, Aizawa H, Okinami S, Nagai H, Hasegawa M, Fukuda T, Green ED, Izuhara K. Identification of pendrin as a common mediator for mucus production in bronchial asthma and chronic obstructive pulmonary disease. *J Immunol* 180: 6262–6269, 2008.
38. Novak I, Young JA. Two independent anion transport systems in rabbit mandibular salivary glands. *Pflügers Arch* 407: 649–656, 1986.
39. O'Reilly CM, Wimpenny JP, Argent BE, Gray MA. Cystic fibrosis transmembrane conductance regulator currents in guinea pig pancreatic duct cells: inhibition by bicarbonate ions. *Gastroenterology* 118: 1187–1196, 2000.
40. Ohana E, Shcheynikov N, Park M, Muallem S. Solute carrier family 26 member a2 (Slc26a2) protein functions as an electroneutral $\text{SO}_4^{2-}/\text{OH}^-/\text{Cl}^-$ exchanger regulated by extracellular Cl^- . *J Biol Chem* 287: 5122–5132, 2012.
41. Pedemonte N, Caci E, Sondo E, Caputo A, Rhoden K, Pfeiffer U, Di Candia M, Bandettini R, Ravazzolo R, Zegarri-Moran O, Galletta LJ. Thiocyanate transport in resting and IL-4-stimulated human bronchial epithelial cells: role of pendrin and anion channels. *J Immunol* 178: 5144–5153, 2007.
42. Pezzulo AA, Tang XX, Hoegger MJ, Abou Alaiwa MH, Ramachandran S, Moninger TO, Karp PH, Wohlford-Lenane CL, Haagsman HP, van Eijk M, Banfi B, Horswill AR, Stoltz DA, McCray PB, Welsh MJ, Zabner J. Reduced airway surface pH impairs bacterial killing in the porcine cystic fibrosis lung. *Nature* 487: 109–113, 2012.
43. Poulsen JH, Fischer H, Illek B, Machen TE. Bicarbonate conductance and pH regulatory capability of cystic fibrosis transmembrane conductance regulator. *Proc Natl Acad Sci USA* 91: 5340–5344, 1994.
44. Proesmans M, Vermeulen F, De Boeck K. What's new in cystic fibrosis? From treating symptoms to correction of the basic defect. *Eur J Pediatr* 167: 839–849, 2008.
45. Quinton PM. Cystic fibrosis: impaired bicarbonate secretion and mucoviscidosis. *Lancet* 372: 415–417, 2008.
46. Quinton PM. Role of epithelial HCO_3^- transport in mucin secretion: lessons from cystic fibrosis. *Am J Physiol Cell Physiol* 299: C1222–C1233, 2010.
47. Reddy MM, Quinton PM. Effect of anion transport blockers on CFTR in the human sweat duct. *J Membr Biol* 189: 15–25, 2002.
48. Reimold FR, Heneghan JF, Stewart AK, Zelikovic I, Vandorpe DH, Shmukler BE, Alper SL. Pendrin function and regulation in *Xenopus* oocytes. *Cell Physiol Biochem* 28: 435–450, 2011.
49. Romero MF, Chen AP, Parker MD, Boron WF. The SLC4 family of bicarbonate (HCO_3^-) transporters. *Mol Aspects Med* 34: 159–182, 2013.
50. Schultz BD. Airway epithelial cells: “bicarbonate in” \neq “bicarbonate out.” *J Physiol* 590: 5263–5264, 2012.
51. Scott DA, Karniski LP. Human pendrin expressed in *Xenopus laevis* oocytes mediates chloride/formate exchange. *Am J Physiol Cell Physiol* 278: C207–C211, 2000.
52. Scott DA, Wang R, Kreman TM, Sheffield VC, Karniski LP. The Pendred syndrome gene encodes a chloride-iodide transport protein. *Nat Genet* 21: 440–443, 1999.
53. Sehgal A, Presente A, Engelhardt JF. Developmental expression patterns of CFTR in ferret tracheal surface airway and submucosal gland epithelia. *Am J Respir Cell Mol Biol* 15: 122–131, 1996.
54. Shan J, Huang J, Liao J, Robert R, Hanrahan JW. Anion secretion by a model epithelium: more lessons from Calu-3. *Acta Physiol (Oxf)* 202: 523–531, 2011.
55. Shan J, Liao J, Huang J, Robert R, Palmer ML, Fahrenkrug SC, O'Grady SM, Hanrahan JW. Bicarbonate-dependent chloride transport drives fluid secretion by the human airway epithelial cell line Calu-3. *J Physiol* 590: 5273–5297, 2012.
56. Shcheynikov N, Yang D, Wang Y, Zeng W, Karniski LP, So I, Wall SM, Muallem S. The Slc26a4 transporter functions as an electroneutral $\text{Cl}^-/\text{I}^-/\text{HCO}_3^-$ exchanger: role of Slc26a4 and Slc26a6 in I^- and HCO_3^- secretion and in regulation of CFTR in the parotid duct. *J Physiol* 586: 3813–3824, 2008.
57. Shen RQ, Finkbeiner WE, Wine JJ, Mrsny RJ, Widdicombe JH. Calu-3—a human airway epithelial cell line that shows cAMP-dependent Cl^- secretion. *Am J Physiol Lung Cell Mol Physiol* 266: L493–L501, 1994.
58. Simpson JE, Schweinfest CW, Shull GE, Gawenis LR, Walker NM, Boyle KT, Soleimani M, Clarke LL. PAT-1 (Slc26a6) is the predominant apical membrane $\text{Cl}^-/\text{HCO}_3^-$ exchanger in the upper villous epithelium of the murine duodenum. *Am J Physiol Gastrointest Liver Physiol* 292: G1079–G1088, 2007.
59. Smith JJ, Welsh MJ. cAMP stimulates bicarbonate secretion across normal, but not cystic fibrosis airway epithelia. *J Clin Invest* 89: 1148, 1992.
60. Song YL, Salinas D, Nielson DW, Verkman AS. Hyperacidity of secreted fluid from submucosal glands in early cystic fibrosis. *Am J Physiol Cell Physiol* 290: C741–C749, 2006.
61. Stewart AK, Yamamoto A, Nakakuki M, Kondo T, Alper SL, Ishiguro H. Functional coupling of apical $\text{Cl}^-/\text{HCO}_3^-$ exchange with CFTR in stimulated HCO_3^- secretion by guinea pig interlobular pancreatic duct. *Am J Physiol Gastrointest Liver Physiol* 296: G1307–G1317, 2009.
62. Tamada T, Hug MJ, Frizzell RA, Bridges RJ. Microelectrode and impedance analysis of anion secretion in Calu-3 cells. *JOP 2 Suppl* 4: 219–228, 2001.
63. Thiagarajah JR, Song YL, Haggie PM, Verkman AS. A small molecule CFTR inhibitor produces cystic fibrosis-like submucosal gland fluid secretions in normal airways. *FASEB J* 18: 875–877, 2004.
64. Thomas JA, Buchsbaum RN, Zimniak A, Racker E. Intracellular pH measurements in Ehrlich ascites tumor cells utilizing spectroscopic probes generated in situ. *Biochemistry* 18: 2210–2218, 1979.
65. Turner RJ, George JN. $\text{Cl}^-/\text{HCO}_3^-$ exchange is present with $\text{Na}^+/\text{K}^+/\text{Cl}^-$ cotransport in rabbit parotid acinar basolateral membranes. *Am J Physiol Cell Physiol* 254: C391–C396, 1988.
66. Walker NM, Simpson JE, Brazill JM, Gill RK, Dudeja PK, Schweinfest CW, Clarke LL. Role of down-regulated in adenoma anion exchanger in HCO_3^- secretion across murine duodenum. *Gastroenterology* 136: 893–901, 2009.